# Pulse-front tilt caused by spatial and temporal chirp

**Selcuk Akturk, Xun Gu, Erik Zeek, and Rick Trebino**

*School of Physics, Georgia Institute of Technology, Atlanta, Georgia 30332-0430, USA*
akturk@socrates.physics.gatech.edu

**Abstract:** Pulse-front tilt in an ultrashort laser pulse is generally considered to be a direct consequence of, and equivalent to, angular dispersion. We show, however, that, while this is true for certain types of pulse fields, simultaneous temporal chirp and spatial chirp also yield pulse-front tilt, even in the absence of angular dispersion. We verify this effect experimentally using GRENOUILLE.



**OCIS codes:** (320.5550) Pulses; (320.7100) Ultrafast measurements

## References and links

1. R. L. Fork, O. E. Martinez, and J. P. Gordon, "Negative Dispersion Using Pairs of Prisms," Opt. Lett. **9**, 150-152 (1984).
2. J. P. Gordon and R. L. Fork, "Optical resonator with negative dispersion," Opt. Lett. **9**, 153-155 (1984).
3. O. E. Martinez, J. P. Gordon, and R. L. Fork, "Negative group-velocity dispersion using refraction," J. Opt. Soc. Am. B **1**, 1003-1006 (1984).
4. Z. Bor, B. Racz, G. Szabo, M. Hilbert, and H. A. Hazim, "Femtosecond Pulse Front Tilt Caused by Angular-Dispersion," Optical Engineering **32**, 2501-2504 (1993).
5. J. Hebling, "Derivation of the pulse front tilt caused by angular dispersion," Opt. and Quantum Electron. **28**, 1759-1763 (1996).
6. C. Dorrer, E. M. Kosik, and I. A. Walmsley, "Spatio-temporal characterization of ultrashort optical pulses using two-dimensional shearing interferometry," Appl. Phys. B **74 [suppl.]**, 209-219 (2002).
7. I. Z. Kozma, G. Almasi, and J. Hebling, "Geometrical optical modeling of femtosecond setups having angular dispersion," Appl. Phys. B **76**, 257-261 (2003).
8. Z. Bor and B. Racz, "Group-Velocity Dispersion in Prisms and Its Application to Pulse-Compression and Traveling-Wave Excitation," Opt. Commun. **54**, 165-170 (1985).
9. O. E. Martinez, "Pulse Distortions in Tilted Pulse Schemes for Ultrashort Pulses," Opt. Commun. **59**, 229-232 (1986).
10. X. Gu, S. Akturk, and R. Trebino, "Parameterizations of Spatial Chirp in Ultrafast Optics," Opt. Commun. (to be published).
11. E. Hecht, *Optics*, 3rd ed. (Addison Wesley Longman, Inc., 1998).
12. A. G. Kostenbauder, "Ray-Pulse Matrices: A Rational Treatment for Dispersive Optical Systems," IEEE J. Quantum Electron. **26**, 1148-1157 (1990).
13. P. O'Shea, M. Kimmel, X. Gu, and R. Trebino, "Highly simplified ultrashort pulse measurement," Opt. Lett. **26**, 932 (2001).
14. R. Trebino, *Frequency-Resolved Optical Gating* (Kluwer Academic Publishers, Boston, 2002).
15. S. Akturk, M. Kimmel, P. O'Shea, and R. Trebino, "Measuring pulse-front tilt in ultrashort pulses using GRENOUILLE," Opt, Express **11**, 491-501 (2003).
16. S. Akturk, M. Kimmel, P. O'Shea, and R. Trebino, "Measuring spatial chirp in ultrashort pulses using single-shot Frequency-Resolved Optical Gating," Opt. Express **11**, 68-78 (2003).
17. K. Varjú, A. P. Kovács, G. Kurdi, and K. Osvay, "High-precision measurement of angular dispersion in a CPA laser," Appl. Phys, B **74**, S259-S263 (2002).
18. K. Varjú, A. P. Kovács, K. Osvay, and G. Kurdi, "Angular dispersion of femtosecond pulses in a Gaussian beam," Opt. Lett. **27**, 2034-2036 (2002).
19. B. S. Prade, J. M. Schins, E. T. J. Nibbering, M. A. Franco, and A. Mysyrowickz, "A Simple Method for the Determination of the Intensity and Phase of Ultrashort Optical Pulses," Opt. Commun. **113**, 79-84 (1995).
20. O. E. Martinez, "Matrix Formalism for Dispersive Laser Cavities," IEEE J. Quantum Electron. **25**, 296-300 (1989).

#4854 - $15.00 US Received 22 July 2004; revised 3 September 2004; accepted 6 September 2004

21. O. E. Martinez, "Matrix Formalism for Pulse Compressors," IEEE J. Quantum Electron. **24**, 2530-2536 (1988).

## 1. Introduction

The space and time dependences of an ultrashort pulse's electric field are often assumed to be separable into independent functions. This assumption fails when coupling occurs between the pulse electric field's space and time dependences, and this is referred to as a spatio-temporal distortion. Such distortions are common in ultrafast optics because the generation, amplification, and manipulation of ultrashort pulses all involve the deliberate introduction and (it is hoped) subsequent removal of massive spatio-temporal distortions. While it is generally desired that the resulting pulse be free of such distortions, improper alignment is common, and as a result, ultrashort pulses are often contaminated with spatio-temporal distortions. Indeed, the broadband nature of ultrashort pulses makes them particularly vulnerable to these distortions. When such pulses are utilized in applications, these distortions often erode temporal resolution, reduce intensity, and cause a wide range of other problems.

The most common such distortion is angular dispersion (AD), which is usually deliberately caused by the use of a dispersive element such as a prism or grating. AD is useful because it yields negative group-velocity dispersion [1-3], and inverted prism and/or grating pairs act as pulse compressors/stretchers. After the second prism or grating, AD is usually zero, but another spatio-temporal distortion remains—spatial chirp (SC)—in which the frequency varies transversely across the beam. Propagation through another inverted pair of prisms or gratings removes the spatial chirp, and in theory, both the resulting AD and SC are then zero. Unfortunately, these devices (and most other devices involving such elements) have strict alignment requirements, and, as a result, some residual AD and/or SC often remain in the output pulse.

Angular dispersion also yields another spatio-temporal distortion: pulse-front tilt (PFT) (see Fig. 1 left). In fact, it is generally thought that AD and PFT are equivalent phenomena. This was proved using geometrical ray-tracing by Bor *et al*. [4] and Hebling [5], in which plane waves are always considered. Another more general proof using Fourier transform was given by Dorrer *et al*. [6]. Specifically, a beam with pulse-front tilt can be written as:

$$E\left(x,z,t\right)=E_{xz}\left(x,z\right)E_{t}\left(t-px\right) \tag{1}$$

where $p$ is the PFT. We have suppressed the $y$-dependence and assumed that, apart from PFT, $E\left(x,z,t\right)$ has no coupling of its coordinates, so it can be separated into $E_{xz}\left(x,z\right)$ and $E\left(t\right)$. (This is a more rigorous expression than that given in Ref. [6].) Simply Fourier-transforming from the $x$-$t$ domain to the $k$-$\omega$ domain and using two applications of the Shift Theorem, we have:

$$\hat{\tilde{E}}\left(k_{x},k_{z},\omega\right)=\hat{\tilde{E}}_{k_{x}k_{z}}\left(k_{x}-p\omega,k_{z}\right)\hat{\tilde{E}}_{\omega}\left(\omega\right) \tag{2}$$

which is a beam with AD. Specifically, $\mathrm{d}k_{x}/\mathrm{d}\omega=p$, or the AD is $\mathrm{d}\theta_{0}/\mathrm{d}\omega=p/k_{0}$, where $\theta_{0}$ is the propagation angle, and $k_{0}$ is the nominal wave-number in vacuum.

While the above proof seems quite fundamental, we show in this work that angular dispersion and pulse-front tilt are *not* equivalent, and we provide an additional (and rather common!) source of pulse-front tilt, in which no angular dispersion occurs. We point out that the "proof" of AD/PFT equivalence only holds for fields of the above form, and our counter-example incorporates a beam with spatial chirp, which cannot be written in the above form.

#4854 - $15.00 US Received 22 July 2004; revised 3 September 2004; accepted 6 September 2004

Specifically, to see how PFT can easily occur in the absence of AD, consider an initially transform-limited, but spatially chirped, finite-size beam—with no angular dispersion—passing through a dispersive medium (see Fig. 1, right). Due to the group-velocity dispersion in the medium, the redder side of the beam emerges from the medium earlier than the bluer side, resulting in PFT in the output beam. Because no AD exists, this obviously violates the well-known AD/PFT equivalence.

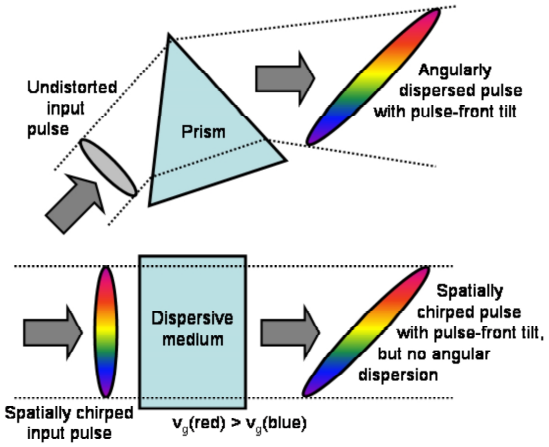


Fig. 1. Two sources of pulse-front tilt. Left: The well-known angular dispersion. Right: The combination of spatial and temporal chirp.

Previous work has considered PFT and AD. Geometrical-optical modeling of AD in ultrashort pulses was performed using plane waves [7]. Bor and Racz [8] showed that position-dependent delays of the pulse front occur at the output of a two-prism pulse compressor, but they did not note the violation of the AD/PFT equivalence. The most comprehensive work on spatio-temporal distortions with dispersive elements is that of Martinez [9], who considered PFT in an angularly dispersed beam with finite beam size. Martinez derived the modified expression of PFT in this case, but did not appear to realize that his finite-beam correction is indeed due to the combined effect of temporal chirp and spatial chirp, both results of beam propagation with AD.

## 2. AD and PFT in the presence of SC

We model both of the effects in Fig. 1 using an expression in the $x$-$\omega$ domain for the electric field of a pulse with linear SC and AD.

$$E(x,\omega) = E(\omega)\exp\left[-\mathrm{i}\frac{k(x-\zeta\omega)^2}{2q}\right]\exp\left(-\mathrm{i}\,k_0\beta\omega x\right) \tag{3}$$

where $k_0$ is the nominal wave-number, $\omega$ is the offset from the center angular frequency, and $q$ is the complex $q$ parameter of a Gaussian beam:

$$q(z) = (z+d) + \mathrm{i}\frac{\pi w^2}{\lambda} = (z+d) + \mathrm{i}\frac{k_0 w^2}{2} \tag{4}$$

#4854 - $15.00 US Received 22 July 2004; revised 3 September 2004; accepted 6 September 2004

where $d$ is the position of the beam waist and $w$ is the spot size. The SC and AD are parameterized by $\zeta \equiv \frac{\mathrm{d}x_0}{\mathrm{d}\omega}$ and $\beta \equiv \frac{\mathrm{d}\theta_0}{\mathrm{d}\omega}$ respectively, where $x_0$ is the beam center position of the $\omega$-component of the beam and $\theta_0$ is the propagation angle of this component.

Throughout this work, we concentrate on spatio-temporal distortions in the *x*-direction only and therefore neglect the beam's *y*-dependence. Generalization to both *x* and *y* dependences is straightforward.

We assume a Gaussian spectrum with linear chirp:

$$E(\omega) = E_0 \exp\left(-\frac{\omega^2 {\tau_0}^2}{4}\right)\exp\left(-\mathrm{i}\frac{\varphi^{(2)}}{2}\omega^2\right) \tag{5}$$

For a well collimated beam, we can write:

$$q(z) \approx q_0(d) = \mathrm{i}\frac{kw^2}{2} \tag{6}$$

Using these expressions, Eq. (3) becomes

$$E(x,\omega) = E_0 \exp\left(-\frac{\omega^2 {\tau_0}^2}{4}\right)\exp\left[-\frac{(x-\zeta\omega)^2}{w^2}\right]\exp\left(-\mathrm{i}\frac{\varphi^{(2)}}{2}\omega^2\right)\exp\left(-\mathrm{i}k_0\beta\omega x\right) \tag{7}$$

Here, we would like to point out, as shown in Ref. [10], there are two related, but different, definitions of spatial chirp. We can either define spatial chirp as the *spatial dispersion* $\zeta \equiv \frac{\mathrm{d}x_0}{\mathrm{d}\omega}$, where $x_0$ is the beam center position of the $\omega$-component, or equivalently define it as the frequency gradient $\upsilon \equiv \frac{\mathrm{d}\omega_0}{\mathrm{d}x}$, where $\omega_0$ is the mean frequency at position $x$. These quantities are not reciprocals of each other, and the relationship between $\zeta$ and $\upsilon$ for Gaussian pulses and beams is

$$\upsilon = \frac{\zeta}{\zeta^2 + \frac{w^2 {\tau_0}^2}{4}} \tag{8}$$

Using the frequency gradient $\upsilon$, Eq. (7) may be rewritten as

$$E(x,\omega) = E_0 \exp\left[-\left(\frac{x}{w'}\right)^2\right]\exp\left[-\frac{(\tau')^2}{4}(\omega-\upsilon x)^2\right]\exp\left(-\mathrm{i}\frac{\varphi^{(2)}}{2}\omega^2\right)\exp\left(-\mathrm{i}k_0\beta\omega x\right) \tag{9}$$

where

$w' = \left(\frac{1}{w^2} - \frac{\upsilon^2 {\tau_0}^2}{4}\right)^{-\frac{1}{2}}$ is the overall beam width, increased from $w$ due to spatial chirp,

$\tau' = \left({\tau_0}^2 + \frac{4\zeta^2}{w^2}\right)^{\frac{1}{2}}$ is the local transform-limited pulse width, increased from $\tau_0$ due to the reduced locally available bandwidth.

After some reorganizing,

#4854 - $15.00 US Received 22 July 2004; revised 3 September 2004; accepted 6 September 2004

$$E(x,\omega) = E_0 \exp\left[-\left(\frac{x}{w'}\right)^2\right]\exp\left[-\mathrm{i}\left(k_0\beta + \frac{\varphi^{(2)}}{2}\upsilon\right)\upsilon x^2\right]$$
$$\times\exp\left[-\frac{(\tau')^2}{4}(\omega-\upsilon x)^2\right]\exp\left[-\mathrm{i}\frac{\varphi^{(2)}}{2}(\omega-\upsilon x)^2\right] \tag{10}$$
$$\times\exp\left[-\mathrm{i}\left(k_0\beta+\varphi^{(2)}\upsilon\right)x(\omega-\upsilon x)\right]$$

The frequency dependence in Eq. (10) is familiar, namely a linearly chirped pulse, and can be easily inversely Fourier-transformed into the time domain:

$$E_0(x,t) = f(x)\exp\left[-\frac{(t-t_0)^2}{\tau^2}\right]\exp\left\{\mathrm{i}\left[\phi^{(1)}(t-t_0)+\frac{\phi^{(2)}}{2}(t-t_0)^2\right]\right\} \tag{11}$$

where:

$$f(x) = \frac{1}{\pi}\left[(\tau')^2 + \mathrm{i}\,2\varphi_2\right]^{-1/2} E_0 \exp\left[-\left(\frac{x}{w'}\right)^2\right]\exp\left(\mathrm{i}\frac{\varphi^{(2)}}{2}\upsilon^2 x^2\right) \tag{12}$$

$$t_0 = \left(k_0\beta + \varphi^{(2)}\upsilon\right)x \tag{13}$$

$$\tau = \left[(\tau')^2 + \frac{4\left(\varphi^{(2)}\right)^2}{(\tau')^2}\right]^{1/2} = \left[\tau_0{}^2 + \frac{4\zeta^2}{w^2} + \frac{4\left(\varphi^{(2)}\right)^2}{\tau_0{}^2 + \frac{4\zeta^2}{w^2}}\right]^{1/2} \tag{14}$$

$$\phi^{(1)} = \upsilon x \tag{15}$$

$$\phi^{(2)} = \frac{\varphi^{(2)}}{\frac{(\tau')^2}{4} + \left(\varphi^{(2)}\right)^2} = \frac{\varphi^{(2)}}{\frac{1}{4}\left(\tau_0{}^2 + \frac{4\zeta^2}{\sigma^2}\right)^2 + \left(\varphi^{(2)}\right)^2} \tag{16}$$

We identify $t_0$ as the pulse-front (maximum intensity contour) arrival time, and the PFT may be characterized by the derivative of $t_0$ with respect to $x$,

$$p \equiv \frac{\mathrm{d}t_0}{\mathrm{d}x} \tag{17}$$

The PFT angle—the angle between the pulse front and the propagation direction $z$—is then given by

$$\tan\psi = pc \tag{18}$$

From Eq. (13), it is easy to see that, for an ultrashort-pulse beam with Gaussian spectrum and Gaussian spatial profile, the PFT is

$$p = p_{\mathrm{AD}} + p_{\mathrm{SC+TC}} \tag{19}$$

where

$$p_{\mathrm{AD}} = k_0\beta \tag{20}$$

#4854 - $15.00 US Received 22 July 2004; revised 3 September 2004; accepted 6 September 2004

$$p_{\mathrm{SC+TC}} = \varphi^{(2)} \upsilon \tag{21}$$

This is the key result of this paper. PFT, in general, consists of two terms. The first term $p_{\mathrm{AD}}$ is the well known angular-dispersion term, as derived by Bor *et al*. [4] and Hebling [5]. The second term $p_{\mathrm{SC+TC}}$ is a PFT effect caused by the combination of SC, which is characterized by the frequency gradient $\upsilon$ and temporal chirp, which is characterized by group-delay dispersion $\varphi^{(2)}$. This new PFT effect is clearly the cause of the PFT in the scenario shown in Fig. 1 (right), in which no AD exists.

This additional source of PFT is not in violation of the proof in Section 1 that purports to show the equivalence of AD and PF. Equations (1)–(2), after all, are simply an exercise in Fourier transforms. Rather, the proof of equivalence is simply not sufficiently general because the forms of Eqs. (1) and (2) specifically preclude the presence of SC in the pulse. Fourier transforming Eq. (1) with respect to *t* yields a field in the *x*-$\omega$ domain of the form:

$$\tilde{E}(x, z, \omega) = E_{xz}(x, z)\, \tilde{E}_{\omega}(\omega) \exp(-\mathrm{i}\, px\omega) \tag{22}$$

But the presence of SC in the form of spatial dispersion requires an expression in the *x*-$\omega$ domain of the form:

$$\tilde{E}(x, z, \omega) = E_{xz}(x - \zeta\omega, z)\, \tilde{E}_{\omega}(\omega) \exp(-\mathrm{i}\, px\omega) \tag{23}$$

that is, some additional coupling of $x$ and $\omega$ beyond the simple complex exponential. An example of this coupling is Eq. (3). The presence of SC in the form of frequency gradient requires an expression in the *x*-$\omega$ domain of the form:

$$\tilde{E}(x, z, \omega) = E_{xz}(x, z)\, \tilde{E}_{\omega}(\omega - \upsilon x) \exp(-\mathrm{i}\, px\omega) \tag{24}$$

Again, this requires coupling of $x$ and $\omega$ beyond the simple complex exponential of Eq. (22).

It is also important to note that these two sources of PFT have subtle physical effects on the pulse, beyond simply tilting the pulse front. AD causes different frequency components to propagate at different angles, resulting in tilt of both the pulse fronts (contours of equal intensity) and the phase fronts (contours of equal phase). On the other hand, simultaneous spatial and temporal chirp tilts the pulse front, while leaving phase fronts of constituent frequencies untilted. This point is very important in the measurement of the two effects. Also, some techniques purport to measure PFT, but in fact measure AD, and vice versa.

### 3. Propagation of ultrashort-pulse beams with angular dispersion and spatial chirp

Equations (10) and (11) give the expressions of the electric field in frequency and time domains at a particular longitudinal position $z_0$. In this section, we propagate the field to an arbitrary position $z$, and discuss how the spatial-temporal coupling parameters, including SC and PFT, evolve. To accomplish this, we use the Fresnel-Kirchoff integral formula [11]:

$$E(x, \omega, z) = \frac{\mathrm{i}}{\lambda z} \int_{-\infty}^{\infty} E(x', \omega, z = 0) \exp\left[ -\frac{\mathrm{i}\pi}{\lambda z} (x - x')^2 \right] \mathrm{d}x' \tag{25}$$

We start from an initial field at $z_0 = 0$,

#4854 - $15.00 US Received 22 July 2004; revised 3 September 2004; accepted 6 September 2004

$$E(x,\omega,z=0)=E(\omega,z=0)\exp\left[-\mathrm{i}\frac{k_0(x-\zeta_0\omega)^2}{2q_0}\right]\exp(-\mathrm{i}k_0\beta\omega x)$$
$$=E_0\exp\left(-\frac{\omega^2\tau_0^{\,2}}{4}\right)\exp\left(-\mathrm{i}\frac{\varphi_0^{(2)}}{2}\omega^2\right)\exp\left[-\mathrm{i}\frac{k_0(x-\zeta_0\omega)^2}{2q_0}\right]\exp(-\mathrm{i}k_0\beta\omega x) \tag{26}$$

Substituting Eq. (26) in Eq. (25), we obtain:

$$E(x,\omega,z)=\frac{\mathrm{i}k_0}{2\pi z}E_0\exp\left(-\frac{\omega^2\tau_0^{\,2}}{4}\right)\exp\left(-\mathrm{i}\frac{\varphi_0^{(2)}}{2}\omega^2\right)$$
$$\times\int_{-\infty}^{\infty}\exp\left[-\mathrm{i}\frac{k_0(x')^2}{2q(0)}\right]\exp\left[-\mathrm{i}k_0\beta\omega(x'+\zeta_0\omega)\right]\exp\left[-\frac{\mathrm{i}k_0}{2z}(x'+\zeta_0\omega-x)^2\right]\mathrm{d}x'$$
$$=\left[\frac{\mathrm{i}k_0}{2\pi z}\frac{q(0)}{q(z)}\right]^{1/2}E_0\exp\left(-\frac{\omega^2\tau_0^{\,2}}{4}\right)\exp\left(-\mathrm{i}\frac{\varphi_0^{(2)}}{2}\omega^2\right)$$
$$\times\exp\left\{\mathrm{i}\frac{k_0z}{2}\frac{q(0)}{q(z)}\left(\frac{x-\zeta_0\omega}{z}-\beta\omega\right)^2-\mathrm{i}k_0\left[\beta\zeta_0\omega^2+\frac{(x-\zeta_0\omega)^2}{2z}\right]\right\} \tag{27}$$

For a well collimated beam, we can write:

$$\frac{q(0)}{q(z)}=\frac{d+\mathrm{i}\frac{k_0w^2}{2}}{z+d+\mathrm{i}\frac{k_0w^2}{2}}=1+\mathrm{i}\frac{2z}{k_0w^2} \tag{28}$$

Equation (27) then simplifies to:

$$E(x,\omega,z)=\left(\frac{\mathrm{i}k_0}{2\pi z}\right)^{1/2}\left(1+\mathrm{i}\frac{2z}{k_0w^2}\right)^{1/2}E_0\exp\left(-\frac{\omega^2\tau_0^{\,2}}{4}\right)\exp\left[-\frac{\mathrm{i}}{2}\left(\varphi_0^{(2)}-k_0\beta^2z\right)\omega^2\right]$$
$$\times\exp\left\{-\frac{\left[x-(\zeta_0+\beta z)\omega\right]^2}{w^2}\right\}\exp(-\mathrm{i}k_0\beta\omega x) \tag{29}$$

Note that this is exactly in the form of Eq. (7), with the spatial dispersion and group-delay dispersion parameters substituted by the *z*-evolved values:

$$\zeta(z)=\zeta_0+\beta z \tag{30}$$

$$\varphi^{(2)}(z)=\varphi_0^{(2)}-k_0\beta^2z \tag{31}$$

The physical meanings of these results are obvious. Equation (30) describes the increase of spatial dispersion with propagation due to AD. As the pulse propagates, different colors in the pulse become increasingly separated from each other. Equation (31) describes the introduction of negative group-delay dispersion (GDD) due to AD, which is the theoretical basis of pulse compressors. Using the evolved values of spatial dispersion and GDD, the

#4854 - $15.00 US Received 22 July 2004; revised 3 September 2004; accepted 6 September 2004

results in the previous section can applied to obtain the evolution of other spatial-temporal coupling parameters, including frequency gradient $\upsilon$ and PFT $p$:

$$\upsilon(z) = \frac{\zeta_0 + \beta z}{(\zeta_0 + \beta z)^2 + \frac{w^2 \tau_0^2}{4}} \tag{32}$$

$$p = k_0 \beta + \left(\varphi_0^{(2)} - k_0 \beta^2 z\right) \upsilon(z) \tag{33}$$

The generalized theory of spatio-temporal coupling in ultrashort-pulse beams can also be derived analogously using the matrix formalism introduced by A. G. Kostenbauder [12] (see Appendix).

## 4. Experiment

In the previous sections, we showed that simultaneous spatial and temporal chirp cause PFT, even in the absence of AD. In this section, we describe an experimental demonstration of these theoretical results. Our experimental setup is shown in Fig. 2. We used a prism pair to introduce SC in the beam. Identical Brewster prisms aligned anti-parallel were used to ensure that angular dispersion was eliminated after the second prism. The beam then entered an imaging spectrometer with the direction of the spatial chirp along the entrance slit. A CCD camera on the exit plane of the spectrometer measured the spatio-spectral intensity profile of the beam. From this trace, we could either measure the slope of the beam center position vs. frequency, which yields the spatial dispersion $\zeta$, or the slope of the center frequency vs. position, which yields the frequency gradient $\upsilon$. The same beam was also sent to a Swamp Optics GRENOUILLE [13,14], which measured both the GDD and the PFT with high sensitivity [15]. (GRENOUILLE also reveals SC [16], but a spatially resolved high-resolution spectrometer measurement has higher sensitivity for SC.) Other sensitive methods of measuring PFT have also been demonstrated [17,18], but they in fact measure AD. As a result, they could not be used for our purposes. Interferometric techniques can also be used to measure PFT [6,19] but we did not prefer them due to their experimental complexity. Our setup (see Fig. 2) introduced constant SC with no AD. Translating one of the prisms in and out of the beam adjusted the temporal chirp in the usual manner.

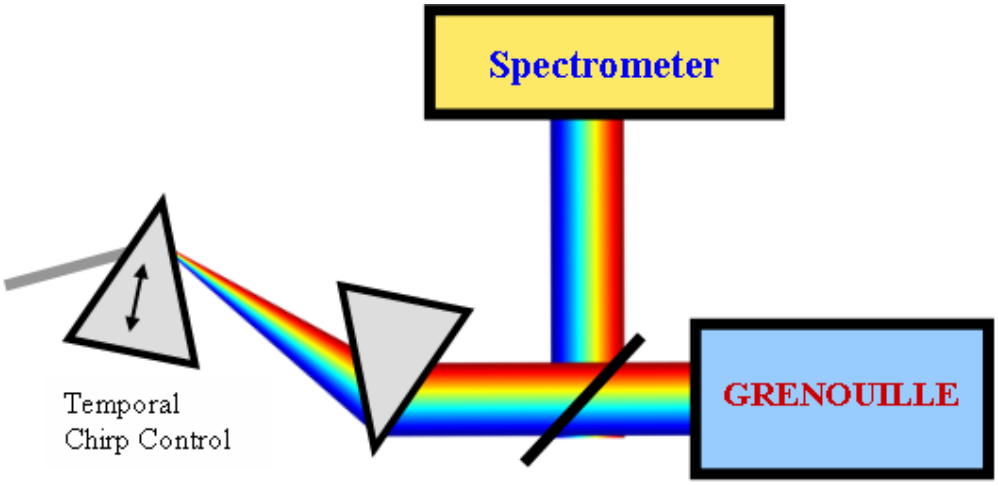


Fig. 2. Apparatus to introduce constant spatial chirp, variable temporal chirp and no angular dispersion.

#4854 - $15.00 US Received 22 July 2004; revised 3 September 2004; accepted 6 September 2004

GRENOUILLE measures the PFT as a shift of the center of the trace along the delay axis [15]. Therefore, by translating the prism in and out of the beam (adding and removing material and hence adjusting the temporal chirp of the output beam), we expect to see a change in the shift of the center of the trace. Figure 3 shows some of the experimental GRENOUILLE traces for different values of temporal chirp. These traces clearly show that, although no AD is present, the beam possesses a significant amount of PFT that results from spatial and temporal chirp. This qualitatively demonstrates our theory.

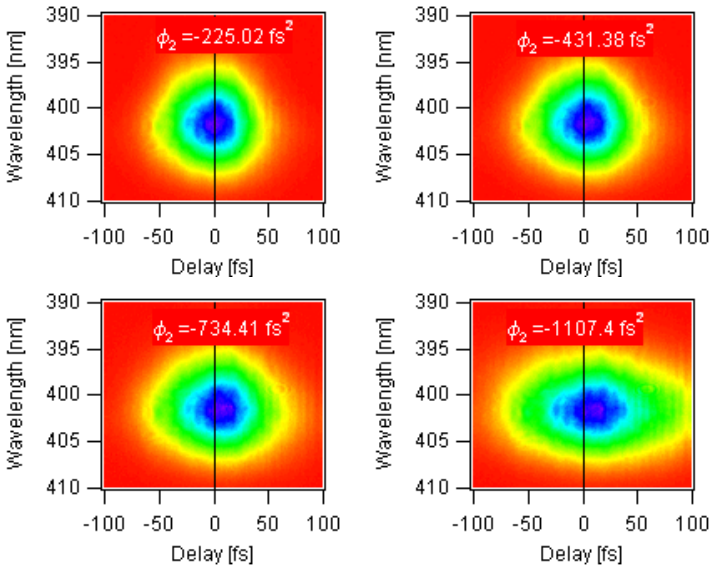


Fig. 3. GRENOUILLE traces of a beam that has a constant spatial chirp and variable temporal chirp. Note that the amount of shift of the center (a measure of pulse-front tilt) increases with increasing temporal chirp.

More quantitatively, Eq. (15) shows that the slope of PFT $p$ vs. GDD $\varphi^{(2)}$ yields the frequency gradient $\upsilon$. Figure 4 shows such a plot. We measured the slope of this plot to be $8.78\times10^{-3}\ \left(\text{rad}\cdot\text{fs}^{-1}\right)/\text{mm}$ $\left(\frac{\mathrm{d}\lambda_0}{\mathrm{d}x}=2.98\ \text{nm/mm}\right)$. The value of the frequency gradient measured by the spectrometer is $8.87\times10^{-3}\ \left(\text{rad}\cdot\text{fs}^{-1}\right)/\text{mm}$ $\left(\frac{\mathrm{d}\lambda_0}{\mathrm{d}x}=3.01\ \text{nm/mm}\right)$, in excellent agreement with the other measurement.

#4854 - $15.00 US
Received 22 July 2004; revised 3 September 2004; accepted 6 September 2004

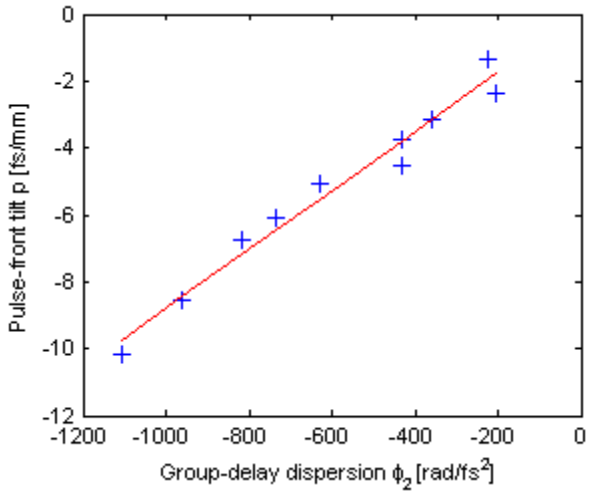


Fig. 4. Experimental measurements (plus-sign symbols) of pulse-front tilt for different amounts of GDD. The red line shows the linear fit.

## 5. Conclusion

In conclusion, we have shown that the equivalence of pulse-front tilt and angular dispersion is valid only for beams without spatial chirp. In the presence of spatial chirp, the combination of spatial and temporal chirp also causes pulse-front tilt. We have derived analytical expressions for ultrashort–pulse beams that possess angular dispersion, spatial chirp and temporal chirp. We verified our theoretical results experimentally using GRENOUILLE.


## Acknowledgments

This material is based upon work supported by the National Science Foundation under Grant No. #ECS-0200223. We are grateful for helpful discussions with A. G. Kostenbauder.


## Appendix

We have shown above that simultaneous temporal and spatial chirp causes PFT even in the absence of angular dispersion. Here, we provide an alternative derivation using the matrix formalism introduced by Martinez [20,21] and extended by Kostenbauder [12].

An optical system that introduces spatial and temporal chirp can be described in terms of a 4×4 ray-pulse matrix as:

$$K = \begin{bmatrix} A & B & 0 & E \\ C & D & 0 & F \\ G & H & 1 & I \\ 0 & 0 & 0 & 1 \end{bmatrix} = \begin{bmatrix} 1 & L & 0 & 2\pi\zeta \\ 0 & 1 & 0 & 0 \\ 0 & -2\pi\zeta/\lambda_0 & 1 & 2\pi\varphi^{(2)} \\ 0 & 0 & 0 & 1 \end{bmatrix} \tag{A1}$$

where $\zeta$ is spatial dispersion and $\varphi^{(2)}$ is the GDD.

Matrix $K$ can be obtained either by calculating the system ray-pulse matrix for a two-prism pulse compressor separated by $L$ or for a fictitious system that introduces only spatial chirp followed by a dispersive slab of thickness $nL$ (where $n = n(\omega)$ is the index of refraction). In both cases, GDD is the total GDD due to both the material and angular dispersions. Note that this approach describes only rays or plane waves (which has the form

#4854 - $15.00 US Received 22 July 2004; revised 3 September 2004; accepted 6 September 2004

given in Eqs. (1) and (2)), so the matrix shows no pulse-front tilt ($K_{31} = \frac{\partial t}{\partial x} = 0$), as we expect.

In order to apply the ray-pulse matrix to a finite-size Gaussian beam, we must use the complex *Q* matrix, as illustrated by Kostenbauder in Ref. [12]. Using this approach, the spatio-temporal electric field is expressed as:

$$E(x,t) = \exp\left\{-\mathrm{i}\frac{\pi}{\lambda_0}\begin{pmatrix} x \\ -t \end{pmatrix}^T Q^{-1}\begin{pmatrix} x \\ t \end{pmatrix}\right\} = \exp\left[-\mathrm{i}\frac{\pi}{\lambda_0}\left(\left(Q^{-1}\right)_{11} x^2 + \left(Q^{-1}\right)_{12} xt - \left(Q^{-1}\right)_{21} xt - \left(Q^{-1}\right)_{22} t^2\right)\right] \tag{A2}$$

The off-diagonal elements of the matrix $Q^{-1}$ indicate spatial-temporal coupling. If we write the magnitude of electric field in terms of the local pulse length and the pulse-front tilt as

$$\left|E(x,t)\right| \propto \exp\left[-\frac{(t-px)^2}{\tau^2}\right] \tag{A3}$$

Equating the magnitude of (A2) and (A3) yields

$$\tau = \left[\frac{\pi}{\lambda_0}\mathrm{Im}\left\{\left(Q^{-1}\right)_{22}\right\}\right]^{-\frac{1}{2}} \tag{A4}$$

$$p = \frac{\pi\tau^2}{2\lambda_0}\mathrm{Im}\left\{\left(Q^{-1}\right)_{12} - \left(Q^{-1}\right)_{21}\right\} = \frac{\mathrm{Im}\left\{\left(Q^{-1}\right)_{12} - \left(Q^{-1}\right)_{21}\right\}}{2\,\mathrm{Im}\left\{\left(Q^{-1}\right)_{22}\right\}} \tag{A5}$$

For an input pulse with no spatio-temporal distortions and flat phase, we have:

$$\left(Q_{\mathrm{in}}^{-1}\right)_{11} = \frac{1}{q} \tag{A6}$$

$$\left(Q_{\mathrm{in}}^{-1}\right)_{22} = \mathrm{i}\frac{\lambda_0}{\pi\tau_0^2} \tag{A7}$$

Then the input Q matrix is:

$$Q_{\mathrm{in}} = \begin{bmatrix} q & 0 \\ 0 & -\mathrm{i}\dfrac{\pi\tau_0^2}{\lambda_0} \end{bmatrix} \tag{A8}$$

The output Q matrix is found by:

$$Q_{\mathrm{out}} = \left\{\begin{bmatrix} A & 0 \\ G & 1 \end{bmatrix} Q_{\mathrm{in}} + \begin{bmatrix} B & E/\lambda_0 \\ H & I/\lambda_0 \end{bmatrix}\right\} \cdot \left\{\begin{bmatrix} C & 0 \\ 0 & 1 \end{bmatrix} Q_{\mathrm{in}} + \begin{bmatrix} D & F/\lambda_0 \\ 0 & 1 \end{bmatrix}\right\}^{-1} \tag{A9}$$

Substituting the elements of *K* from Eq. (A1) into (A9), we obtain:

#4854 - $15.00 US Received 22 July 2004; revised 3 September 2004; accepted 6 September 2004

$$Q_{\text{out}} = \begin{bmatrix} q+L & \dfrac{2\pi\zeta}{\lambda_0} \\ -\dfrac{2\pi\zeta}{\lambda_0} & \dfrac{2\pi\varphi^{(2)}}{\lambda_0} - \mathrm{i}\dfrac{\pi\tau_0^2}{\lambda_0} \end{bmatrix} \tag{A10}$$

Inverting this matrix yields:

$$Q_{\text{out}}^{-1} = \begin{bmatrix} \dfrac{\lambda_0\left(\varphi^{(2)} - \dfrac{\mathrm{i}}{2}\tau_0^2\right)}{\varphi^{(2)}(L+q)\lambda_0 + 2\pi\zeta^2 - \dfrac{\mathrm{i}}{2}(L+q)\lambda_0\tau_0^2} & -\dfrac{\lambda_0\zeta}{\varphi^{(2)}(L+q)\lambda_0 + 2\pi\zeta^2 - \dfrac{\mathrm{i}}{2}(L+q)\lambda_0\tau_0^2} \\ \dfrac{\lambda_0\zeta}{\varphi^{(2)}(L+q)\lambda_0 + 2\pi\zeta^2 - \dfrac{\mathrm{i}}{2}(L+q)\lambda_0\tau_0^2} & \dfrac{1}{2\pi}\dfrac{(L+q)\lambda_0^2}{\varphi^{(2)}(L+q)\lambda_0 + 2\pi\zeta^2 - \dfrac{\mathrm{i}}{2}(L+q)\lambda_0\tau_0^2} \end{bmatrix} \tag{A11}$$

For a well collimated beam, we can approximate:

$$q(L) = L + q \approx \mathrm{i}\frac{\pi w^2}{\lambda_0} \tag{A12}$$

Therefore,

$$Q_{\text{out}}^{-1} = \begin{bmatrix} \dfrac{\lambda_0}{\pi}\dfrac{2\varphi^{(2)} - \mathrm{i}\,\tau_0^2}{4\zeta^2 + w^2\tau_0^2 + \mathrm{i}\,2\varphi^{(2)}w^2} & -\dfrac{2\lambda_0}{\pi}\dfrac{\zeta}{4\zeta^2 + w^2\tau_0^2 + \mathrm{i}\,2\varphi^{(2)}w^2} \\ \dfrac{2\lambda_0}{\pi}\dfrac{\zeta}{4\zeta^2 + w^2\tau_0^2 + \mathrm{i}\,2\varphi^{(2)}w^2} & \mathrm{i}\dfrac{\lambda_0}{\pi}\dfrac{w^2}{4\zeta^2 + w^2\tau_0^2 + \mathrm{i}\,2\varphi^{(2)}w^2} \end{bmatrix} \tag{A13}$$

Using Eqs. (A4) and (A5), we find

$$\tau = \left[\tau_0^{\,2} + \frac{4\zeta^2}{w^2} + \frac{4\left(\varphi^{(2)}\right)^2}{\tau_0^{\,2} + \dfrac{4\zeta^2}{w^2}}\right]^{1/2} \tag{A14}$$

$$p = \frac{\varphi^{(2)}\zeta}{\zeta^2 + \dfrac{1}{4}w^2\tau_0^{\,2}} \tag{A15}$$

which are identical to the results we obtained in the main text.

#4854 - $15.00 US Received 22 July 2004; revised 3 September 2004; accepted 6 September 2004